Available online at www.sciencedirect.com
SCIENCE DIRECT®
Polymer 44 (2003) 3561–3578
polymer
www.elsevier.com/locate/polymer

Dynamic mechanical and tensile properties of poly(*N*-vinyl pyrrolidone)–poly(ethylene glycol) blends

Mikhail B. Novikov[a], Alexandra Roos[b], Costantino Creton[b], Mikhail M. Feldstein[a,*]

[a]*A.V. Topchiev Institute for Petrochemical Synthesis, Russian Academy of Sciences, 29, Leninsky prospekt, 119991, Moscow, Russian Federation*
[b]*Laboratoire de Physico-Chimie Structurale et Macromoléculaire, Ecole Supérieure de Physique et de Chimie Industrielles de la ville de Paris (ESPCI), 10, rue Vauquelin, 75231, Paris, Cedex 05, France*

Received 10 October 2002; received in revised form 30 January 2003; accepted 10 February 2003

Abstract

Mechanical properties of miscible blends of high molecular weight poly(*N*-vinyl pyrrolidone) (PVP) with a short-chain, liquid poly(ethylene glycol) (PEG) of molecular weight 400 g/mol have been examined as a function of PVP–PEG composition and degree of hydration. The small-strain behavior in the linear elastic region has been evaluated with the dynamic mechanical analysis and compared with the viscoelastic behavior of PVP–PEG blends under large strains in the course of uniaxial drawing to fracture and under cyclic extension. A strong decoupling between the small-strain and the large strain properties of the blends has been observed, indicative of a pronounced deviation from rubber elasticity in the behavior of the blends. This deviation, also seen on tensile tests under fast drawing, is attributed to the peculiar phase behavior of the blends and the molecular mechanism of PVP–PEG interaction. Nevertheless, for the PVP blend with 36% PEG, under comparatively low extension rates, the reversible contribution to the total work of deformation up to $\varepsilon = 300\%$ has been found to be maximum at around 70%, while the blends containing 31 and 41% PEG behave rather as an elastic–plastic solid and a viscoelastic liquid, respectively.
© 2003 Elsevier Science Ltd. All rights reserved.

Keywords: Poly(*N*-vinyl pyrrolidone); Poly(ethylene glycol); Blends

1. Introduction

Pressure-sensitive adhesives (PSA) are commonly used in a variety of applications because of their ease of application, low toxicity and versatility [1]. Adhesion and viscoelasticity are the macroscopic properties of polymers. They involve numerous processes at a microscopic and molecular level. The PSAs are polymers or polymeric composites, which are capable of forming a strong adhesive bond with a substrate surface over a short contact time of 1–2 s by application of a very slight pressure. At long timescales, the PSA polymers can behave almost like very viscous liquids, whereas at shorter timescales, they deform like soft, elastic solids and can store elastic energy which is then released upon detachment. The characteristic timescales are affected by chemical composition, chain length, and supramolecular structure [2].

A considerable amount of research work has been performed on the correlation between mechanical properties of PSAs and their adhesive performance [1–5]. Moreover, an abundant literature exists arguing that adhesive properties of PSAs can be predicted from their linear viscoelastic properties [6–11]. According to the Dahlquist criterion for stickiness, the elastic modulus of a PSA should be around 10^5 Pa on the time scale of the bonding process (ca. 1 s) [12]. Chu reported the correlation between the storage modulus of the adhesive, G', and its peel adhesion and tack [13]. Dale et al. reported a good correlation between peel strength and the value of the loss tangent, tan δ [14].

To be a PSA, the polymer should possess a high segmental mobility (a common property of liquids), facilitating the formation of adhesive bond, coupled with solid-like resistance to flow in order to prevent an early failure of the adhesive joint when the debonding stress is applied [1]. This latter property is typical of cured rubbers or solid polymers which do not exhibit fluid behavior. The optimum combination of adhesive performance properties is therefore difficult to provide. It is therefore not surprising

* Corresponding author. Tel.: +7-095-955-4372; fax: +7-095-230-2224.
E-mail address: mfeld@ips.ac.ru (M.M. Feldstein).

0032-3861/03/$ - see front matter © 2003 Elsevier Science Ltd. All rights reserved.
doi:10.1016/S0032-3861(03)00132-0

that of the thousands of polymers and polymeric blends, that have been prepared and evaluated over the years, there are currently only a few classes of PSAs: natural rubber, butyl rubber, synthetic polyisoprene, styrene–butadiene random and block copolymers, polyacrylates, polyurethanes, and silicones [1]. It is noteworthy that all the PSA are based on hydrophobic elastomers with low glass transition temperatures ranging from −120 to −30 °C, which are usually increased by adding tackifying resins.

However, for a range of specific needs, in particular for medical applications, fewer hydrophilic PSA materials are currently available. The poly(*N*-vinyl pyrrolidone) (PVP)–poly(ethylene glycol) (PEG) adhesive has been designed to make up this deficiency and to serve as a skin contact adhesive and drug reservoir in transdermal patches for controlled drug delivery [15–17].

As has been recently established with the Optical Wedge Microinterferometry technique, glassy PVP easily soluble in PEG oligomers ($M_w < 1000$ g/mol), forming a single phase, stable solution [18,19]. At the same time, the PVP is found to be immiscible with higher molecular weight PEG ($M_w \geq 1000$ g/mol) [19]. This behavior is indicative of the contribution of proton-donating hydroxyl groups at the ends of PEG short chains to the miscibility with PVP. The latter contains only electron-donating reactive carbonyl groups in the repeat units. Actually, according to the FTIR spectroscopy data, the PVP–PEG miscibility is due to hydrogen bonding of both terminal PEG hydroxyls to the complementary carbonyl groups in the PVP monomer units [20,21]. Because the PEG chains bear two terminal hydroxyl groups, they act as hydrogen-bonding, labile and transient crosslinkers between the longer PVP macromolecules. Although every monomer unit in the PVP macromolecule contains one reactive carbonyl group, only nearly 20% of them are crosslinked through the shorter chains of PEG-400 in a network H-bonded complex within a wide range of PVP–PEG compositions [21–23]. This behavior characterizes the PVP–PEG H-bonded complex as exhibiting a non-equimolar stoichiometry and network supramolecular structure.

Owing to the appreciable length and flexibility of the PEG chains, they create a space within the PVP–PEG network and provide the coupling of the high cohesive strength of an H-bonded complex and a large free volume. The latter was determined for the PVP–PEG blends with positron annihillation lifetime spectroscopy (PALS) [24]. In turn, the network imparts to the blend a rubber-like elasticity that has been established with rheological measurements [20], whereas the free volume leads to increased molecular mobility of the blend, which was evaluated in terms of PEG self-diffusion coefficient with a pulsed field gradient NMR (PFG NMR) method [25,26]. In this way, both major requirements accounting for pressure sensitive adhesion have been obtained, and it is therefore of no wonder, that the pressure sensitive adhesion appears in the PVP–PEG blends, within a narrow range of composition, in vicinity 36 wt% PEG-400.

The adhesion in the PVP–PEG system has been examined as a function of the blend composition and of the degree of hydration using the peel [27] and probe tack tests [28]. As has been shown in the first of these two papers, both plasticizers, PEG and water, behave as tackifiers (enhancers of adhesion) in the blends with glassy PVP. However, the tackifying effect of PEG is appreciably stronger than that of sorbed water. Blend hydration enhances adhesion for the systems that exhibit adhesive type of debonding (at PEG content less than 36 wt%). However, the same amounts of sorbed water is also capable of decreasing the adhesion in the blends containing more than 36% PEG, where a cohesive mechanism of adhesive joint failure is typical. The PVP–PEG blend with 36% PEG couples both the adhesive and cohesive mechanisms of bond rupture (i.e. the fibrillation of adhesive polymer under debonding force and a predominantly adhesive locus of failure [27]).

The micromechanics of adhesive joint failure for PVP–PEG hydrogels has been found to involve the fibrillation of the adhesive polymer, followed by fibrils stretching and fracturing as their elongation attains 1000–1500% [27]. The peel force to rupture the adhesive bond of PVP–PEG blends obeyed reasonably well the Kaelble equation, derived originally for conventional hydrophobic pressure sensitive adhesives [29]. The major deformation mode upon peeling the PVP–PEG adhesive from a standard substrate is in extension, and direct correlations have been established between the composition behavior of peel strength and that of the total work of viscoelastic strain to break the PVP–PEG films under uniaxial drawing [27].

As the data of probe tack testing has shown [28], at low debonding rates the debonding took place through the formation of a fibrillar structure, while at high debonding rate the debonding was brittle. This transition was attributed to the breakage and reformation of hydrogen bonds between PVP units and OH groups on the PEG during the large strain of the polymer chains in elongation. The comparison between the tack properties of the PVP–PEG adhesives and their linear viscoelastic properties showed a very strong decoupling between the small-strain and the large strain properties of the adhesive indicative of a pronounced deviation from rubber elasticity in the deformation behavior of the blends. As a result, it was impossible to predict even qualitatively the adhesive properties of hydrophilic PVP–PEG adhesives from G' and G'' data in stark contrast with conventional PSAs based on hydrophobic rubbers [28]. Therefore, it is logical to suppose that different molecular mechanisms contribute to the adhesive and mechanical properties of the PVP–PEG blends under small and larger deformations.

The goal of our investigation is to elucidate the role played by water and PEG in controlling the small and large strain properties of the blends in order to interpret better

their adhesive properties. In order to do so, we have investigated the small-strain oscillatory shear properties, the tensile properties at constant crosshead velocity and the hysteresis properties in the large strain regime.

2. Materials and methods

2.1. Preparation of samples

PVP (Kollidon K-90), $M_w = 1,000,000$ g/mol, $M_n = 360,000$ g/mol, glass transition temperature $T_g = 178$ °C (BASF), and PEG of molecular weight 400 g/mol, $T_g = -70$ °C (Carbowax Sentry NF, Union Carbide Corp.) were used as received. Both polymers are hygroscopic and the degree of their hydration, evaluated by the weight loss under drying at 105 °C, is taken into account to prepare physical blends containing from 20 to 41 wt% of PEG-400. Depending on the relative humidity (RH) of the surrounding atmosphere, the PVP degree of hydration ranged from 6 to 8 wt%, while the PEG contained less sorbed water (0–1 wt%).

Polyisobutylene (PIB, Vistanex LM, $M_w = 13,300$ g/mol) and DURO-TAK 34-4230 pressure sensitive adhesive (PSA), consisting of a plasticized styrene–isoprene–styrene (SIS) block copolymer, mixed with tackifier and filler, were obtained from the National Starch and Chem. Corp.

2.2. Dynamic mechanical analysis

The dynamic mechanical properties of the adhesives in the linear viscoelastic regime were measured on a parallel plate rheometer RDA II from Rheometrics.

The PVP–PEG solutions in ethanol were poured in teflon moulds (2 cm-deep) and remained at room temperature during 7 days in order to evaporate most of the solvent. The resulting films (1–1.5 mm-thick) were then dried 3 h under vacuum, at 65 °C. The water content of the adhesive films was then equilibrated by leaving the samples at room temperature in dessiccators under constant levels of RH (RH = 53 and 100%) for 6 days and overnight, respectively. The required RH = 53% was provided by a sulfuric acid solution with $d = 1.29$ g/cm^3. After the samples were conditioned and before testing, the water content was measured on a selected sample by weight loss after thoroughly drying in vacuum, 90 °C. While the sample upon drying contained about 1 wt% of water, for conditioned samples the films contained 11 and 40 wt% water, respectively.

Pellets (diameter 8 mm) were finally taken out of these films with a circular punch. At room temperature, the sample was positioned in the rheometer and kept 15 min under a slight pressure in order to ensure a good adhesion between the polymer blend and the rheometer plates. The temperature was then gradually decreased to the lowest temperature of the experiment.

For the blends containing 31 and 36 wt% PEG, we varied the temperature from −20 to 130 °C, in 5 °C steps from −20 to 80 °C and 10 °C steps from 90 to 130 °C. The frequencies varied from 0.05 to 100 rad/s (10 points per decade) for each temperature below 25 °C, and from 0.05 to 500 rad/s for higher temperatures. For the blend containing 41 wt% PEG, we varied the temperature from −50 to 0 °C, in 5 °C steps, and the frequencies were varied from 0.05 to 100 rad/s (10 points per decade). The amplitude of deformation was chosen to be in the linearity regime of the elastic modulus G' over the whole range of temperatures. For our PVP–PEG blends this zone corresponded to a deformation varying from 0.1 to 1% depending on the temperature.

Finally master curves as a function of temperature were constructed by applying the time–temperature equivalence. The reference frequency of 1 Hz was chosen for all the blends examined, while for the most liquid blend containing 41% PEG the highest temperature where the measurement was possible was 0 °C.

2.3. Tensile testing

The films of PVP–PEG blends were prepared by dissolving PVP and PEG in a common solvent (ethyl alcohol) then casting the solution onto the siliconized surface of a polyethylene terephthalate (PET) PEBAX-600 release linear (60 μm in thickness) and finally evaporating the solvent at ambient temperature and RH for 3 days until a constant weight was attained. In the casting solution, the concentration of PVP in ethyl alcohol was about 40 wt%. The solvent removal was verified by FTIR spectroscopy, observing the lack of methylene group stretching vibrations at 2974 and 1378 cm^{-1} in the IR spectrum. The hydration of freshly prepared PVP–PEG blends, containing 36 wt% of PEG-400, averaged 6.5 ± 0.8 wt%. From this point on the term 'hydrogels' is used to designate equilibrium hydrated PVP–PEG blends.

A uniform thickness of the PVP–PEG hydrogel films subjected to tensile tests was obtained by using BYK-Gardner film casting knife (AG-4300 Series). This instrument consists of an adjustable clearance film applicator blade supported by two end plates. The bottom edge of the drawdown blade was adjusted to the desired height by means of two micrometers located on top of the applicator. The resolution to which the micrometer could be positioned was about 5 μm. The casting solution was poured in front of the applicator between the end plates. The instrument was then moved at a slow and uniform rate across the surface of the PEBAX-600 release liner backing, which was perfectly flat, until the viscous PVP–PEG casting solution had all been applied and any surplus had been drawn off the panel at the end of a wet film path. The wet film thickness (1.2–1.4 mm) was approximately twice the required value of dry

film thickness (500–700 μm). Upon drying, the PVP–PEG adhesive films were covered by the second sheet of the PEBAX-600 release liner and cut with a die cutter, producing rectangular samples of 1×3 cm^2.

The films of PIB and SIS adhesives of 500–700 μm in thickness were prepared by pressing the polymers between two sheets of the PEBAX-600 release liner in a mold formed by two parallel flat stainless plates of 2×4 cm in size at 70 °C for 20 min, followed by cooling the samples in the mold to ambient temperature and relaxation for 24 h. The cutting of the PIB and SIS films was provided by the same procedure as described above for the PVP–PEG films.

Tensile strain–stress behavior of the adhesive films was studied with an Instron 1222 Tensile Tester at ambient temperature. Dumbbell-shaped samples of the total length of 21 mm with a nip-to-nip distance of 10 mm were cut from rectangular films of 0.5–0.7 mm in thickness. The width of a necked region was 5 mm. The tensile strength of the samples was determined at fixed cross head speed ranging from 10 to 100 mm/min, 10 N full scale load. The nominal tensile stress was defined as a stretching force normalized by the original cross-section area of the sample. In order to evaluate a true tensile stress, the following assumptions were made:

(1) The material deforms uniformly along the entire sample length. This has been established to be the case for the uniaxial drawing of PVP–PEG adhesive hydrogel.
(2) Both the total volume and the density of the sample are constant in the course of elongation. Then, the true tensile stress (σ_T) relates to the nominal one (σ_N) by the expression (1) [30]:

$$\sigma_T = \sigma_N(1 + \varepsilon) \quad (1)$$

The ultimate tensile strength being the maximum force applied (to breaking) divided by the cross-sectional area of the sample. Elongation at break is calculated by dividing the distance that the crosshead of the Instron tensile had traveled to sample break by the original length of the sample. All reported stress–strain curves were reproduced in replicate experiments, varying less than 10%.

Extension–retraction cycles were recorded under loading a polymer film to a specified elongation of $\varepsilon = 3.0$ at a rate of 10 mm/min, followed by immediate unloading of the specimen with the same rate until zero load. Elongation–retraction cycles were repeated trice, and the specimens were never allowed to relax in the course of the triple extension–retraction loading. The elongation values at the points where retraction stress achieved zero were taken as a plastic (unrecoverable) residual strain (ε_p). Respectively, the recoverable (elastic) strain was $\varepsilon_e = 3.0 - \varepsilon_p$. Although the stress–strain curves are mainly shown in this work in terms of nominal tensile stress, those were recalculated into the values of true tensile stress, and all the quantities, presented below, relate to the true values.

2.4. Other test methods

Optical anisotropy of the uniaxilly stretched PVP–PEG films was studied using a Polam L 213 microscope with a 250× magnification.

The TM-DSC heating thermograms were measured with a 2820 Modulated Differential Scanning Calorimeter (TA Instruments). In the TM-DSC apparatus, the samples were first quench cooled with liquid nitrogen from ambient temperature to −150 °C at a cooling rate of 10 °C/min, subjected to isothermal annealing at this temperature and then heated up to 220 °C at a rate of 5 °C/min. The constant heating rate was superimposed with a temperature modulation with a period of 60 s and an amplitude of ±0.796 °C. The respective T_gs were recorded at half-height of the relevant heat capacity jumps. All reported values are the average of replicate experiments varying less than 1–2%. In order to avoid the superposition of the glass transition response with other thermal events, in the TM-DSC tests the heating scans were analyzed by the TA Universal Analysis software using the reversible heat flux only. All the TM-DSC measurements were performed with the samples hermetically sealed in aluminum pans in order to avoid water evaporation. It was important to ensure a perfect contact between the pans and the heating cell and to have very flat pans.

3. Results and discussion

3.1. Dynamic mechanical properties of PVP blend with 36% PEG-400

According to the results of the Peel and Probe Tack Test measurements [27,28], the blend of high molecular weight PVP with liquid short-chain PEG-400 (36 wt%) exhibits the best adhesion. A viscoelastic characterization method, such as dynamic mechanical analysis (DMA) provides a more accurate method of determining the moduli of the PVP–PEG hydrogel. Fig. 1 shows a typical example of the DMA data obtained at a frequency of 1 Hz for the PVP–PEG blend containing 36 wt% PEG. As the temperature is increased, the storage modulus, G', gradually decreases. Simultaneously, viscous dissipation, which is represented by the loss modulus, G'', also decreases. The G'', maximum is usually closely associated with the glass transition temperature, T_g. The ratio between G'', and G', represented by tan δ reaches a peak within a transition region slightly above the T_g, implying therefore that the material is the most viscoelastic at this tan δ peak temperature.

At first glance, the PVP–PEG blend displays the G' and G'', behavior, which is typical of the high molecular-weight polymers used as pressure-sensitive-adhesives, with a

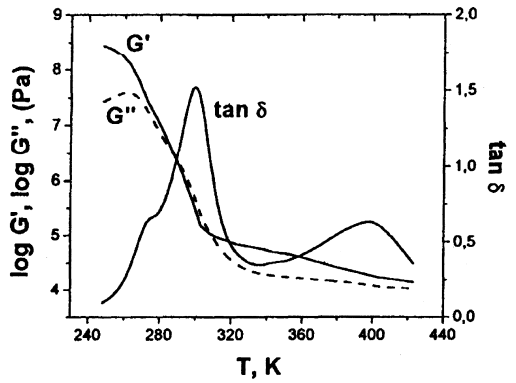

Fig. 1. Master curves of the dynamic shear moduli, G' and G'', and tan δ as a function of temperature for adhesive PVP blend with 36 wt% PEG-400, containing 11% of sorbed water. $\varpi_{ref} = 1$ Hz.

glassy region, a transition region and a higher-temperature plateau region. However, a close observation of the G' and G'', curves reveals a range of peculiarities that is only observed for PVP–PEG PSA.

Typically, at a deformation rate of 1 Hz and at ambient temperature, the value of G' for a PSA lies in the range 0.01–0.1 MPa [31]. The value of G' for the 36% PEG is more in the range 3–5 MPa, a value clearly incompatible with the well-known Dahlquist's criterion for tackiness [12], which specifies that an adhesive loses its tack if its elastic modulus at 1 Hz is higher than about 0.1 MPa. Also typical PSA's are used in a temperature range corresponding to the beginning of the high-temperature rubbery plateau or the end of the transition region [7,11], while the 36% PEG blend has been found to be tacky in a region corresponding to the center of the transition region [27,28].

The storage modulus, G', measures the elasticity of the adhesive. The loss modulus, G'', is on the other hand associated with energy dissipation during deformation. The greater the G'' value relative to G', the more dissipative is the adhesive [32]. The G''/G' ratio, defined as the loss tangent, tan δ, is the balance of viscous/elastic behavior. Tan $\delta = 1$ is a limiting value. Above this value the adhesive is generally considered as a viscoelastic fluid while below this value, the adhesive can be considered as a viscoelastic solid. Typical values of tan δ for conventional PSA's range from 0.1 (styrene–isoprene–styrene blockcopolymer [32,33]) to 0.7 (acrylic PSA [34,35]). In contrast to this behavior of classical rubber-based PSA's, typical G' values for swollen bioadhesive hydrogels based on chemically cross-linked PVP have been reported to range from 3×10^3 to 8×10^4 Pa, while relevant G'' values vary between 1×10^2 and 1×10^4 depending on the degree of swelling [36].

As follows from the data shown in Fig. 1, the value of tan δ is about 1.25 for the PVP–PEG adhesive hydrogel at a temperature 293 K. This value is obviously atypical with respect to the classical PSA's. The found value indicates that, based on the tan δ data the PVP–PEG adhesive is much more dissipative than classical PSA's and behaves rather like a liquid, whereas based on the G' data it is stiffer and provides appreciable cohesion, in comparison with conventional PSA's. Although coupling the liquid-like fluidity with cohesive toughness is a characteristic feature of all the PSA's, in our system this property has been found to result from the molecular mechanism of PVP–PEG interaction [20,21,27]. Probably, while hydrogen bonding between PVP and PEG causes enhanced cohesive strength of the adhesive material (revealed by the high G' value), the location of reactive groups at the ends of PEG chains leads to a large free volume and enhanced molecular mobility (which result in the high G' and tan δ values [24,37,38]). Note, however, that at high temperature, tan δ remains below 1 and the material does not flow. This is consistent with the requirement of low creep under low levels of stress.

Another distinguished feature of the PVP–PEG adhesive is also a multimodality of the tan δ curve (Fig. 1), which shows a shoulder at 273 K (tan $\delta = 0.67$), a peak at 298 K (tan $\delta = 1.57$), and a maximum at 403 K (tan $\delta = 0.65$). This character results in turn from the peculiar phase behavior of the PVP–PEG blends. The phase state of PVP–PEG blends throughout the entire compositional range has been the subject of a thorough examination [18–23,37,39–41]. Although no evidences of phase separation in undeformed films have been observed on a scale of 100 nm and larger [18,19,23], the DSC scans do reveal two distinct glass transitions within the composition range between 20 and 50 wt% PEG [23]. Relevant transition temperatures, T_g, are plotted in Fig. 2 along with the temperatures of the tan δ peak and shoulder versus the content of PEG-400. The composition dependence of the upper T_g value has been shown to follow reasonably the well known Fox equation [42] suggesting the PVP–PEG miscibility and the formation of a homogeneous blend [23]. At the same time, the lower T_g was attributed to the formation of a stoichiometric network complex due to H-bonding of PVP carbonyls to complementary hydroxyl groups at both ends of PEG short chains [23]. In this way, the two T_g-phases have been postulated to possess the same composition but different

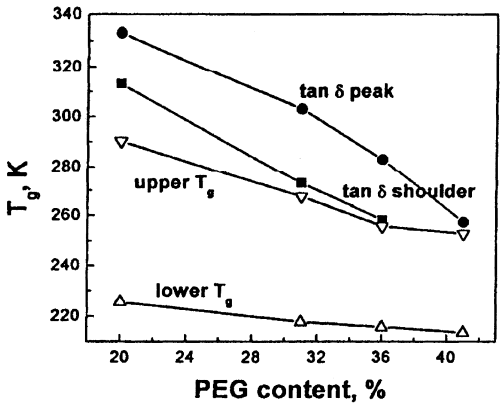

Fig. 2. Dependence of glass transition temperature and the temperatures of the tan δ peak and shoulder on the composition of PVP–PEG blends.

physical properties due to a difference in the PVP–PEG interaction mechanism (uncrosslinked PVP units H-bonded to hydroxyl groups at PEG chains having their opposite terminal group free of bonding in the upper T_g-phase, and the PVP units crosslinked through PEG chains by simultaneous formation of two H-bonds via both terminal hydroxyls in the lower T_g-phase) [23].

Comparing Figs. 1 and 2, it is clear that while both transitions are observed in DSC and in DMA, they are highly shifted in temperature. If the reference frequency is decreased to 0.05 Hz the tan δ curve is shifted toward a lower temperature so that the temperature of the tan δ shoulder corresponds to the lower T_g value established by DSC. However, the tan δ shoulder, peak and maximum are differently affected by the change in frequency. The lower the frequency, the more pronounced are the tan δ shoulder and high temperature maximum, whereas the amplitude of the middle temperature peak of the tan δ is only slightly affected by the change in the reference frequency. This implies different interaction mechanisms underlying these three thermal transitions. The Tan δ peak is supposed to be associated with the upper T_g-phase and does not relate to the PVP–PEG H-bonded network. Two other transitions are thought to be associated with the PVP–PEG network complex formation. The tan δ shoulder corresponds to the lower T_g phase (network complex) [23]. The tan δ maximum at 403 K is caused by vanishing of a shear yield stress [20] due to the rupture of the H-bonded network, which have been recently established to occur at this temperature due to the rupture of PVP–PEG H-bonds [43].

As is obvious from the temperature profile of tan δ, presented in Fig. 1, the PVP blend with 36% PEG exhibits the best adhesion (at 293–308 K [15,16,27,28]) in the vicinity of the tan δ peak (298 K). This behavior is absolutely unique among the PSA's described to date. To gain an insight into the nature of this phenomenon, we have to consider the mechanism of PVP–PEG PSA deformation and to relate it to the mechanism of PVP–PEG interaction under applied stress. Since the major mode of PSA deformation in the course of adhesive joint failure is extension [27,28], it is reasonable to employ a simple and illustrative tensile test for this purpose.

3.2. Uniaxial tensile drawing of PVP–PEG adhesive hydrogel

Fig. 3 shows the effect of the drawing rate upon the stress–strain behavior to break the PVP–PEG hydrogel, containing 36% PEG and exhibiting the highest adhesion [27,28]. In general, the type of stress–strain curves obtained for the PVP–PEG adhesive hydrogel in Fig. 3 is typical of lightly crosslinked high molecular weight polymers [44]. Under an applied tensile stress, the Hooke's Law region occurs first, when the abrupt growth of the stress is accompanied by comparatively small elongation values (up to $\varepsilon \approx 0.5$). Beyond this region, the polymer softens and

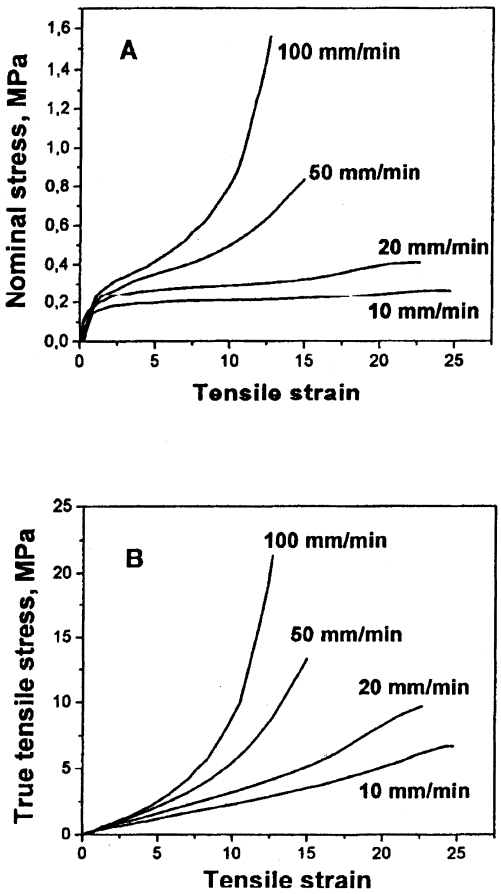

Fig. 3. Stress–strain curves to break the PVP–PEG hydrogel, containing 36 wt% of PEG-400 and 8–9% of water, at drawing rates ranging from 10 to 100 mm/min. (A) Nominal tensile stress. (B) True tensile stress.

the slope of the stress–strain curves decreases becoming apparently linear once again. At comparatively high elongations, the slopes of the curves rise again (strain hardening due to the finite extensibility of the polymer chains). Eventually, fracture occurs. The fracture is characterized by its characteristic stress and strain, which are also called ultimate strength (σ_b), and elongation at break (ε_b).

The stress–strain curves in Fig. 3 are informative on the variation of material resistance to tensile straining under mechanical stress in elongation. The Young's modulus can be determined as the slope of the linear region of the stress–strain curves at very small elongations ($\varepsilon \rightarrow 0$). Since under these conditions, the polymer can be regarded as not disturbed from an equilibrium state, the Young's modulus is often considered as a material constant characterizing polymer elasticity. Beyond this region, the slope of the stress–strain profiles becomes non-linear and depends not only on the sample elasticity, but also on the deformation conditions. It should be noted, however, that because of the deformation of the sample near the grips, the absolute value of the Young's modulus is not very reliable and depends on the exact set-up used and geometry of the test sample.

The transition between the initial region of linear elastic deformation and that of strain softening in Fig. 3 has been shown to be due to the processes of polymer structure rearrangements under mechanical stress. At the moment where stress is applied ($\varepsilon = 0$), the orientation of the polymer chains is still either random, or equilibrium ordered [37], but in any case the structure is isotropic. Under tensile stress the orientation of polymer segments occurs along the axis of drawing, which is ascertained by the appearance of optical anisotropy in polarized light within the region of the onset of elongational flow ($\varepsilon > 0.5-1.0$). The prevalent orientation of PVP long chains in an uniaxially stretched film facilitates the elongational flow of adhesive polymer and results in strain softening.

3.3. Impact of drawing rate on tensile and fracture properties of PVP–PEG adhesive blend

We now discuss the effect of drawing rate on the stress–strain behavior and fracture of PVP–PEG hydrogel. Under comparatively low extension rates (with the rates of 10 and 20 mm/min that correspond to the initial deformation rates of 0.017 and 0.033 s^{-1}), the stress–strain curves have a form characteristic of viscoelastic liquids and ductile, uncured rubbers. At higher drawing rates (50 and 100 mm/min, or 0.083 and 0.167 s^{-1}) they become closer to slightly crosslinked elastomers that deform tightly. The most remarkable feature of the uniaxial drawing of the PVP–PEG hydrogen-bonded network is that the ductile-tight transition occurs very abruptly, within a very narrow range of initial deformation rate between 0.033 and 0.083 s^{-1}. The narrow range of ductile-tight transition in Fig. 3 has been shown to correspond very well to the rapid transition from a tacky, fibrillar failure to a non-tacky and non-fibrillar failure in probe tack test [28]. The latter occurred in the range of debonding rates between 5 and 10 μm/s.

For the PVP–PEG hydrogel the tackiness is most pronounced at lower extension rates, whereas at higher deformation rates it behaves as a non-tacky polymer. This conclusion is also in a good agreement with the results of probe tack testing [28]. The PVP–PEG adhesive has been shown to have a high adhesion energy at low debonding rates, but a good release at high rates of debonding.

3.4. Comparison with other pressure sensitive adhesives

Fig. 4 displays the peculiarities of the tensile stress–strain behavior of PVP–PEG H-bonded network complex in comparison with that of two typical PSA polymers: highly tacky, uncrosslinked low molecular weight PIB, and elastic SIS block copolymer, which is crosslinked physically through glassy polystyrene domains. The latter is filled with relevant tackifier to yield a blend coupling high tack with perfect elasticity and adhesion. Under all drawing rates employed, the shape of stress–strain curves for SIS

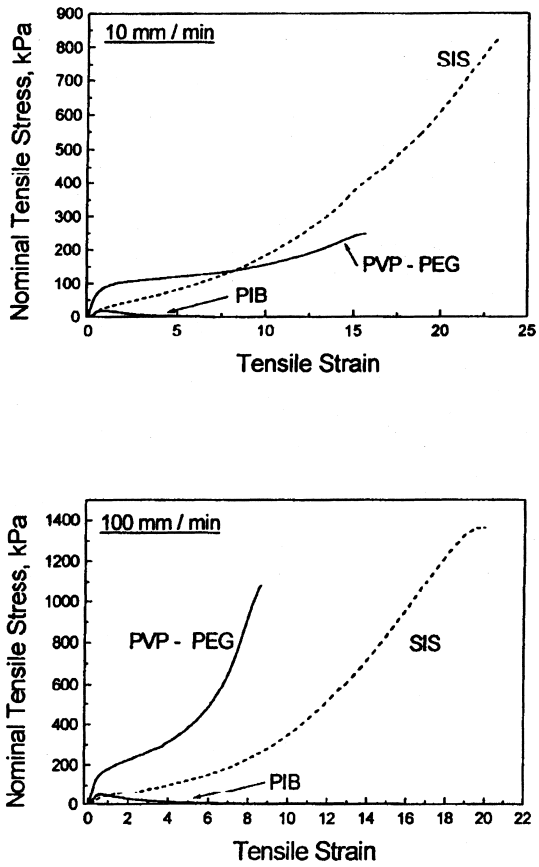

Fig. 4. Stress–strain curves to break the PVP–PEG (36%), PIB and SIS block copolymer (DURO-TAK) adhesives at extension rates of 10 and 100 mm/min.

adhesive is typical of lightly crosslinked elastomers, whereas that of PIB is typical for viscous liquids. In contrast, at low extension rates the shape of the PVP–PEG hydrogel stress–strain curves is intermediate and exhibits a balance between viscous and elastic contributions. The former reveals itself by a relatively high elongation at break value, whereas the latter is evidenced by the increasing level of stress required to deform the adhesive film. Another distinctive feature of the PVP–PEG hydrogel is the high value of the Young's modulus, which implies that the PVP–PEG blend is highly structured in its equilibrium state prior to the application of mechanical stress and resists strongly to deformation.

At high extension rate (100 mm/min), the shape of the PVP–PEG hydrogel stress–strain curve becomes closer to that of a crosslinked elastomer (Fig. 4). Under identical elongation values, the slope of stress–strain curve for PVP–PEG H-bonded complex is always higher than those of the SIS and PIB adhesives. At the same time, the ductility (associated with high elongation at break values) is less pronounced for the PVP–PEG adhesive, than for both hydrophobic PSA's. Comparison of the data presented in Figs. 3 and 4 clearly shows the fact that the 10-fold increase in drawing rate affects the

ductile-tight behavior of the hydrogen bonded PVP–PEG adhesive to a much greater extent than in conventional hydrophobic adhesives. In other words, the ductile-tight transition in the SIS and PIB-based adhesives is much wider than that in PVP–PEG blends.

Cohesive toughness of ductile polymers can be evaluated by the total area enclosed under the stress–strain curve. It is the total work, W_b, that must be done to deform and break the polymer. Specifically, it is a fracture energy per unit volume of material. Much like the W_b quantity, the ultimate tensile strength, σ_b, is a measure of cohesive strength of the material. However, the latter represents the work of fracture and does not include the energy dissipated in the course of deformation. The value of maximum elongation at break, ε_b, which characterizes a process of elongational flow, may be regarded as an indirect measure of polymer tackiness. The ε_b value has been established to vary in proportion to the free volume within the polymer [48]. Fig. 5 plots the W_b, σ_b and ε_b quantities versus extension rate for the PVP–PEG adhesive. While the σ_b and ε_b values are monotonous increasing and decreasing functions of extension rate, the total work of viscoclastic deformation to break, W_b, passes through a maximum at the rate of 20 mm/mm. Let us recall that the work of adhesion of PVP–PEG blend is highly affected by debonding rate, reducing dramatically under faster debonding [27,28]. Let us then try to quantify in an approximate way this behavior by using the values of the σ_b/ε_b ratio. This quantity can be interpreted physically as an average modulus of the adhesive at the moment of fracture. We obtain, that the values of the σ_b/ε_b ratio are 0.27, 0.55, 0.96, and 1.83 MPa at the extension rates of 10, 20, 50 and 100 mm/min, respectively (Table 1). The former two values obey fairly reasonably the Dahlquist's criterion of tack [12], and really in the course of extension with the rate of 50 mm/min and higher the PVP–PEG adhesive exhibits no tack. Thus, while the Dahlquist's criterion is invalid for PVP–PEG adhesive blends under small strains, it still appear to hold as an empirical criterion in the region of large deformations.

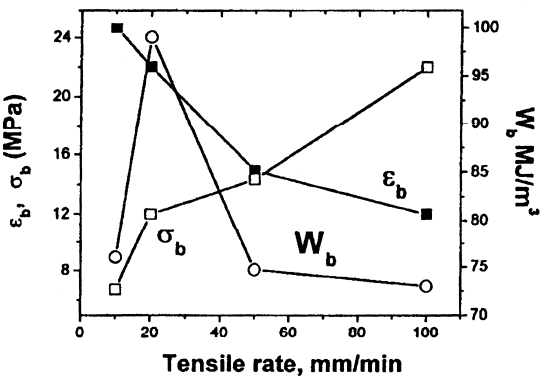

Fig. 5. Impact of drawing rate on the total work to deform and break the PVP–PEG adhesive film, W_b, the ultimate tensile strength, σ_b, and the break elongation, ε_b.

Table 1
The Young's modulus, E, and the σ_b/ε_b ratio for the PVP–PEG blends

PEG content (%)	Degree of hydration (%)	Drawing rate (mm/min)	E (MPa)	σ_b/ε_b (MPa)
36	8–9	10	0.35	0.27
		20	0.47	0.55
		50	0.65	0.96
		100	0.71	1.83
31	8–9	20	0.60	1.06
34			0.47	0.86
36			0.47	0.57
39			0.47	0.30
41			0.34	0.083
36	3	20	1.66	1.30
	4.5		0.42	0.94
	6.5		0.21	0.30
	11		0.16	0.25

3.5. Effect of PEG content and degree of hydration on mechanical properties of PVP–PEG blends

With the increase in PEG concentration in the blend, at a fixed temperature of 20 °C and a frequency of 1 Hz, both the G' and G'' moduli decrease from 31.6 to 0.01 MPa (for 20 and 41% PEG, respectively), following the pattern shown in Fig. 1 for the blend with 36% PEG. Fig. 6 displays the effect of PEG content on the temperature dependence of tan δ for PVP–PEG blends containing 11% of sorbed water. If the 36% PEG is the reference blend (as a reminder this blend displayed the best adhesive behavior both in peel [27] and probe tack tests [28]), the PVP blends with 31 and 20% PEG show a similar behavior shifted by about 15° and 50°, respectively, towards the higher temperatures while the blend with 41% PEG displays a maximum dissipation at a temperature shifted by 45° towards lower values.

As is supposed above (see Section 3.1), the middle temperature peak and lower temperature shoulder in the tan δ curve could be associated with the upper and lower temperatures of glass transitions, established by a TM-DSC method [23]. Let us now go back to Fig. 2, where the temperatures of the shoulder and the peak on tan δ curves,

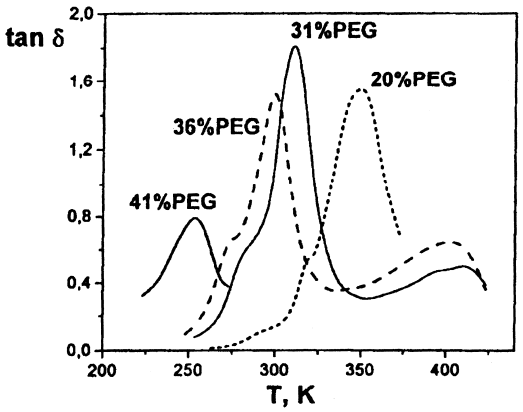

Fig. 6. Master curves of tan δ as a function of temperature for the three blends with 11 wt%. water, $w_{ref} = 1$ Hz.

along with relevant T_g values, are plotted versus PEG concentration in blend. While the temperature interval between the upper and lower T_g values is gradually decreased with the increase in PEG content, the curves for the shoulder and the peak of tan δ run almost in parallel. Thus, while according to the DSC data the PVP blends containing from 20 to 45% PEG reveal some primary evidence of a two-phase structure, the results of DMA indicate that the two distinct kinds of structures, responsible for the peak and shoulder of tan δ, respectively, co-exist rather within a single phase. A similar conclusion is also derived from a closer analysis of the TM-DSC data [23]: the lower and upper T_g-phases have been supposed to have the same composition but disparate physical properties owing to different types of PVP–PEG H-bonding. Following this concept, we can hypothesize that the shoulder on the tan δ curves relates to the PVP macromolecules crosslinked by H-bonding through shorter PEG chains. The middle-temperature tan δ peak reflects then the contribution of uncrosslinked PVP chains, plasticized with PEG that form H-bonds through one terminal group only.

In a similar manner, the increase in blend hydration from 1 to 40% water content causes the shift of the G' and G'' curves towards lower temperatures. The tan δ curves of the PVP–PEG (36%) blends with 1, 11 and 40% water at a reference frequency of 1 Hz are shown in Fig. 7. It is quite clear that the water molecules act as a potent plasticizer and shift the rheological behavior in temperature in an analogous way to the PEG. However, the characteristic feature of the effect of water is that for the dry blends (1% water) the tan δ peak is not preceded by the lower temperature shoulder. This fact is also easily explicable within the concept of crosslinked stoichiometric PVP–PEG complex formation. Actually, as is shown in Ref. [23], the formation of crosslinked PVP–PEG complex (lower T_g-phase) occurs within a homogeneous PVP–PEG mixture (upper T_g-phase) and is controlled by the upper T_g value.

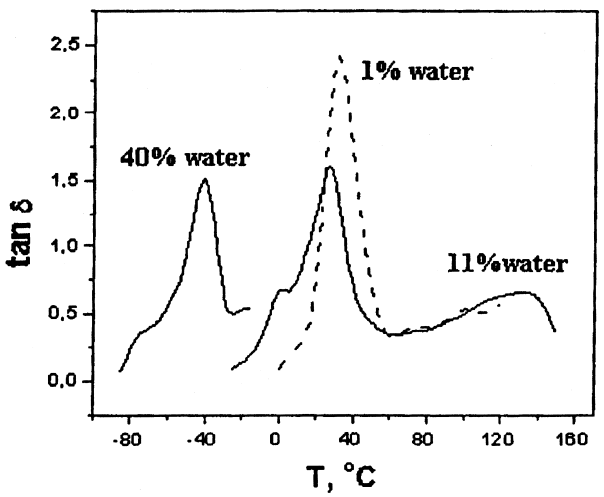

Fig. 7. Master curves of tan δ as a function of temperature for the 36% PEG blend with three different levels of hydration. $w_{ref} = 1$ Hz.

Because the less hydration the higher the T_g, the complex formation is essentially suppressed in dry blends compared to those of moderate degree of hydration.

Another distinctive property of the master curves shown in Fig. 7 is a different effect of water content on tan $\delta = G''/G'$ in the blends of comparatively lower (1–11%) and higher degrees of hydration (40% water). Indeed, the effect of hydration on the dry blends involves mainly the decrease in amplitude of the tan δ peak, whereas the peak temperature decreases comparatively slightly. In contrast, under higher hydration levels the water sorption results in significant shift of tan δ peak towards lower temperatures, while the peak amplitude remains practically unaffected. This means that in dry blends the water contributes mainly to the increase in elasticity modulus G' compared to the loss modulus G'' at the frequency corresponding to the peak of tan δ, while its plasticizing effect (defined as a drop in T_g) is only slightly pronounced. At higher hydration degrees the plasticizing effect of water is predominant.

This difference in the way water affects mechanical properties has been also observed in the adhesive behavior of PVP–PEG systems. In dry blends the water enhances peel adhesion, while in the blend containing more than 11% of water the adhesion is reduced with hydration [27]. As has been shown with DSC, there is no freezing water in PVP–PEG blends while the content of water is lower than 25%. At higher degrees of hydration (more than 25%), unbound (crystallizing) water appears in the blends [41]. Based on this fact we can conclude that the decrease in tan δ in dry blends is due to bound water, whereas the shift of tan δ peak towards lower temperatures is mainly due to the effect of free water that is accumulated in the blends under high hydration.

Similar conclusions follow directly from the tensile test results presented in Figs. 8 and 9. However, the sample containing 40% of sorbed water was too liquid to be tested. Both solvents—PEG-400 and water—are good plasticizers for PVP, and their effects on mechanical properties of the PVP–PEG blends are akin to that of the drawing rate

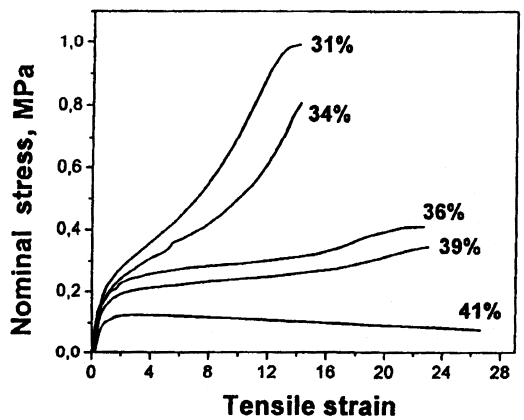

Fig. 8. Tensile stress–strain curves to break the PVP–PEG blends, containing 31, 34, 36, 39, and 41 wt% of PEG-400 at 8–9% degree of hydration. Drawing rate is 20 mm/min.

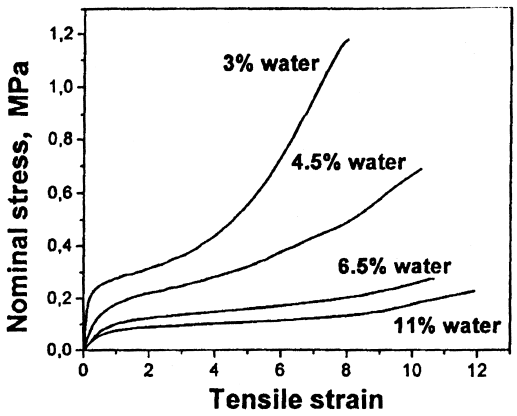

Fig. 9. Impact of water content in PVP blends with 36 wt% of PEG-400 on tensile stress–strain curves to deform and break the PVP–PEG hydrogels under uniaxial drawing with a rate of 20 mm/min.

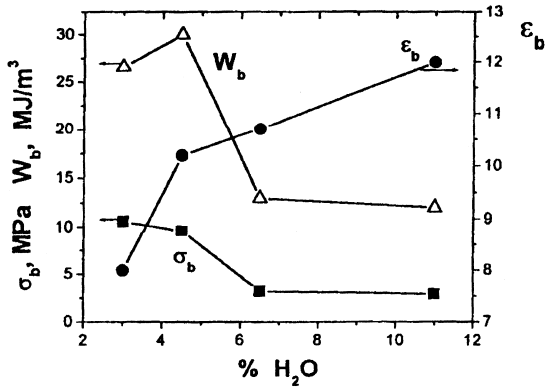

Fig. 11. Effect of water content in PVP–PEG (36%) adhesive hydrogel on the total work of viscoelatic deformation to break the PVP–PEG film, W_b, the ultimate tensile strength, σ_b, and the break elongation, ε_b. Drawing f rate is 20 mm/min.

(compare Figs. 3, 8, and 9). It is worthy of note that under comparatively slow drawing (with a rate of 20 mm/min) the transition from ductile to tight deformation type occurs in a fairly narrow range of PEG content, between 36 and 34% PEG (Fig. 8). In adhesive behavior, this range of PEG concentration corresponds to the transition from fibrillar type of adhesive joint failure (36% PEG and higher) to the brittle-like fracture without fibrillation of the adhesive [27, 28]. Both transitions are shifted toward higher PEG content if the extension or debonding rate are increased.

Figs. 10 and 11 compare the effects of PEG-400 and water on the tensile stress–strain curves of the PVP–PEG blends. The addition of both plasticizers—PEG and water—results in the increase of the elongation at break. However, with the increase in PEG concentration the value of ε_b increases linearly (Fig. 10), whereas the same plot for the effect of water reveals a faster growth of ε_b in dry blends than in hydrated compositions (Fig. 11). For PVP blends containing less than 36% of PEG, the ultimate tensile strength, σ_b, is comparatively high and practically unaffected by PEG content. In contrast, at PEG concentrations higher than 36% the σ_b value declines rapidly with PEG amount (Fig. 10). At the same time, water decreases

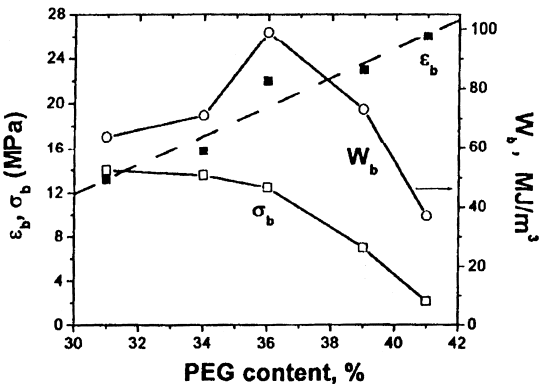

Fig. 10. The total work of viscoelatic deformation to break the PVP–PEG film, W_b, the ultimate tensile strength, σ_b, and the break elongation, ε_b, as a function of PEG concentration in blends. Extension rate is 20 mm/min.

smoothly the cohesive strength of the blends, expressed in terms of the σ_b quantity (Fig. 11). In this way, although PEG induces a plasticization of glassy PVP, it couples the properties of plasticizer at small strains and an enhancer of cohesive strength at large strains, which dominate within different composition regions. At a PEG content below the composition of the PVP–PEG blend, which provides the best adhesion (36 wt% [27,28]), the rise in PEG concentration enhances both the cohesive toughness (ultimate strength to break) and the ductility (break elongation) of adhesive polymer, indicating that PVP crosslinking through H-bonding via terminal hydroxyl groups at PEG short chains is accompanied also by a plasticization effect. At PEG concentrations higher than 36 wt%, the PEG behaves only as a plasticizer, decreasing the cohesive toughness and increasing maximum elongation at fracture. The effect of adding PEG to the adhesive provides a direct experimental confirmation of the earlier established step-wise mechanism of PVP dissolution in liquid PEG [23]. The behavior of water in the PVP–PEG hydrogels has on the other hand a typical plasticizing effect, decreasing E, but leaving unchanged the large strain behavior. The value of the total work of viscoelastic deformation to break the PVP–PEG adhesive hydrogels, W_b, tends to decrease with water content, especially at hydration levels higher than 5% (Fig. 11). In contrast, the dependence of W_b on PEG content (Fig. 10) correlates well with both peel [27] and probe tack adhesion [28], and reveals a maximum at 36% PEG concentration for the blend showing the best adhesion.

Fig. 12 compares the mechanisms of plasticization of water and PEG-400 in the linear-elastic region at small elongations. The value of the elasticity modulus is a monotonous decreasing function of the degree of PVP–PEG hydration which tends to its limiting value upon achieving 7% content of water. At the same time, the plasticizing effect of PEG on PVP is more pronounced in the blends containing less than 33 and more than 39% of PEG-400. According to the concept of the formation of a PVP–PEG stoichiometric network complex [23], the first region

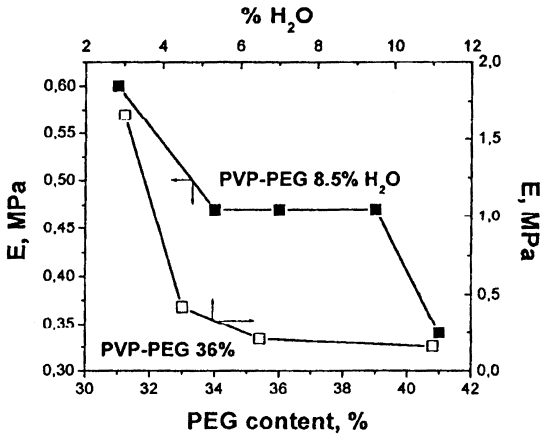

Fig. 12. Comparative effects of PEG and water content on the value of the Young's modulus, E, in PVP–PEG blends under drawing with the rate of 20 mm/min.

corresponds to the stage of crosslinking the PVP chains into the H-bonded network. The second region is related to the stage of gradual swelling of the H-bonded stoichiometric complex in excess PEG-400 which acts as a solvent within this region.

It is quite obvious from Figs. 8–12 that water acts as a plasticizer at a local level and essentially modifies the values of small-strain modulus E, leaving large-strain behavior untouched, while the PEG content affects dramatically the large-strain behavior.

As has been shown in Section 3.4 of this paper, the σ_b/ε_b ratio has a sense of average tensile modulus at the point of polymer fracture (at large deformations). These values are listed for the PVP–PEG blends of various compositions and degrees of hydration in Table 1 along with the Young's modulus, E, that refers to the linear elastic region at small elongations. By this means, comparing the E and σ_b/ε_b values (shown in Table 1) we are able to establish that $E \sim \sigma_b/\varepsilon_b$ only for the blends containing 36% PEG and more so under slow drawing conditions at the rates of 20 and 10 mm/min. In other words, the PVP–PEG system demonstrates a rubber-like viscoelastic behavior mainly under ductile straining. In all other instances the PVP–PEG system demonstrates two very different moduli (for small and large strains, respectively).

For rubbery polymers at small elongations the uniaxial tensil modulus, E, relates to the shear modulus, G, by an equation $E = 3G$. However, comparing the values of small strain tensile moduli in Table 1 with the values of shear moduli found with DMA we see that for PVP–PEG blends $E < G$. In our opinion this abnormal behavior of the PVP–PEG system is not only due to a lot of uncertainty on the measurements of ε at small strains, but also due to a high tensile compliance of ordered H-bonded structure based on long PVP chains oriented along the direction of stretching. This structure is easily formed under uniaxial tensile stress at comparatively small elongations, but does not exist under three-dimensional shear stress.

Another important conclusion that follows directly from the analysis of the σ_b/ε_b values presented in Table 1 refers to the applicability of the Dahlquist's criterion to characterize the tack of PVP–PEG blends. Comparing the results of the evaluation of adhesion in PVP–PEG blends to the data listed in Table 1, we can see that all the blends exhibiting the values of $\sigma_b/\varepsilon_b \leq 0.57$ MPa are always tacky, while the tensile modulus, E, reveals no unequivocal correlation with tackiness. Thus, in contrast to conventional PSA's, the adhesive behavior of PVP–PEG system is controlled by its viscoelastic properties in the region of large strains and at the point of fracture under applied tensile stress. Since the σ_b quantity is a direct characteristic of cohesive toughness, and the ε_b has been shown to be proportional to the fraction of free volume [24,27,45], the σ_b/ε_b ratio outlines a specific balance between the high energy of cohesion and the large free volume as a factor controlling the pressure sensitive adhesion at a molecular level. The found critical magnitude of the σ_b/ε_b ratio (≈ 0.57 MPa and lower), is evidently on the upper border or above the value established by Dahlquist for conventional PSA's [12].

3.6. Cyclic uniaxial stretching of the PVP–PEG films

In order to estimate the relative elastic and plastic contributions to the viscoelastic behavior of the PVP–PEG system under large tensile strain, we subjected the PVP–PEG films to uniaxial cyclic drawing. At the comparatively low extension rate of 10 mm/min, the PVP–PEG hydrogels deform relatively uniformly (see Figs. 3, 8, and 9), and the elongation $\varepsilon = 3.0$ can be therefore taken as a standard tensile strain value during the cyclic uniaxial tension tests. Fig. 13 demonstrates the cyclic stress–strain behavior for PVP blends with 36 wt% of PEG-400 that contain 11% of sorbed water. Being stretched to the $\varepsilon_{max} = 3.0$ elongation, and then drawn back with the same deformation rate, a sample recovers 74% of its strain during the first retraction, achieving a residual elongation of $\varepsilon_{RES} = 0.8$. The strain recovery is defined as a ratio of recoverable strain ($\varepsilon_{REC} = \varepsilon_{max} - \varepsilon_{RES}$) to the full tensile strain ($\varepsilon_{max} - \varepsilon_0$) in the course of an extension–retraction cycle. The ε_{RES} value

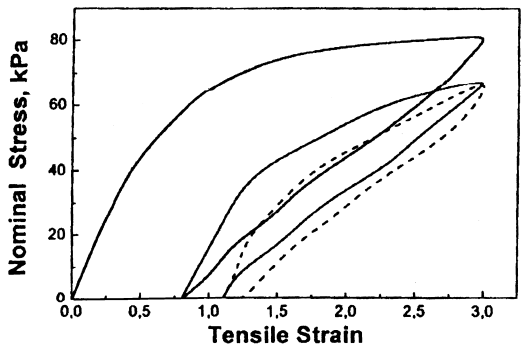

Fig. 13. Extension–retraction behavior of PVP blend containing 36 wt% of PEG-400 and 11 wt% of water under deformation rate of 10 mm/min.

does not characterize an equilibrium plastic strain upon cyclic loading, because if a specimen is allowed to relax at zero stress in the tensile tester immediately following each cyclic test, it continues recovering its length further.

Upon the second cycle, the specimen length achieves a residual strain value of $\varepsilon_{RES} = 1.1$, and thus recovers 86% of its tensile deformation (Fig. 13). After the third cycle, the sample shows 92% strain recovery. Thus, the strain recovery is improved with each extension–retraction cycle, and this behavior is most likely due to the orientation of PVP chains along a drawing direction. In this way, the sample becomes 'trained' during preceding strain cycle, and capable to store more elastic energy in the process of following deformations. This effect is analogous to that found earlier for crosslinked elastomer filled with carbon-black particles [46].

As a polymer film is stretched uniaxially to a predetermined standard elongation value ($\varepsilon = 3.0$) and the tester is then switched from extension to retraction regime, the stress falls immediately by a value of $\Delta\sigma$ from its maximum to a some residual value (σ_{RES}). This behavior is much more easily observable for relatively dry blends (3.5% of water) and those containing a comparatively small amount of PEG-400, which demonstrate a tight type of extension and a brittle-like fracture (Figs. 14 and 15). The σ_{RES} value governs the retraction process. The higher the σ_{RES}, the less the ε_{RES} and the greater the ε_{REC} and strain recovery upon the retraction. Every extension–retraction cycle has been shown to obey this general rule for the PVP–PEG systems.

An area within hysteresis loop (H) is the amount of mechanical energy, that is irreversibly converted into heat during the deformation cycle. This is given by the sum of two integrals: the total work of viscoelastic deformation (W_T) during extension and the work of elastic recovery

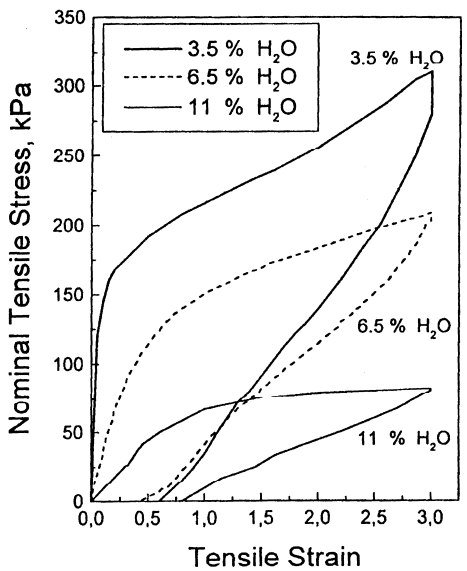

Fig. 14. Effect of PVP–PEG blend hydration on the stress–strain behavior during the first extension–retraction cycle for PVP blends with 36 wt% of PEG-400 at deformation rate of 10 mm/min.

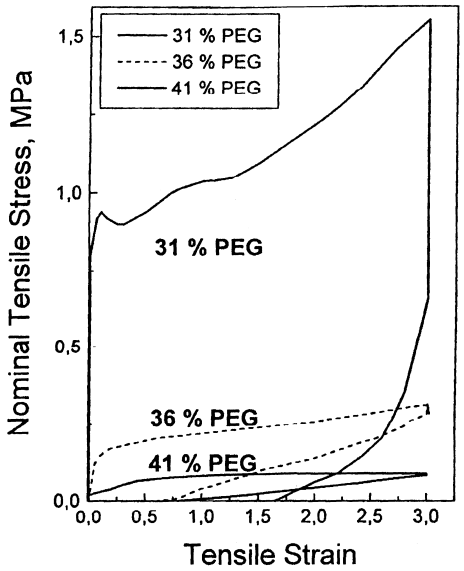

Fig. 15. Effect of PEG content on a single extension–retraction cycle stress–strain curves for PVP–PEG blends, containing 4.5 wt% sorbed water. Deformation rate is 10 mm/min.

under retraction (W_E) :

$$H = W_T + W_E = \int_{\varepsilon_0}^{\varepsilon=3} \sigma \, d\varepsilon + \int_{\varepsilon=3}^{\varepsilon_{RES}} \sigma \, d\varepsilon \qquad (2)$$

The latter term in Eq. (2) is negative.

As follows from the extension–retraction behavior shown in Fig. 13 and Table 2, the hysteresis loop diminishes with increasing number of cycles, but does not vanish completely. Polymer ductility grows with each following extension–retraction cycle, as is evidenced from Fig. 13 by the increase in strain softening. The total work of tensile strain under polymer drawing to a standard elongation value of $\varepsilon = 3$ (W_T) and the work of elastic strain recovery in the course of retraction (W_E) exhibit a reduction with the increasing number of cycles (Table 2). The W_E/W_T ratio defines the elastic contribution to the total deformation work per elongation–retraction cycle. If the $W_E/W_T \geq 0.5$, the behavior of polymer is predominantly elastic.

Indeed, as is evident from the data shown in Table 2 and Fig. 16, with increasing content of both plasticizers, PVP and water, the W_E/W_T quantity increases, passing through a maximum in the first stretching–retraction cycle at 36% amount of PEG and 6.5% water concentration. For PVP blends with 36% PEG, the elastic contribution is always greater than that of dissipated energy. Thus, for PVP–PEG (36%) blend of 11% degree of hydration, the elastic contribution increases from 54.7% in the first cycle to 67.9% and 71.2% under the second and third cyclic straining. For comparison, for SIS-based the DURO-TAK 34-4230 pressure sensitive adhesive the elastic contribution to the total work of viscoelastic deformation is found to be 77.0 and 89.5% in the first and second extension–retraction cycle, respectively.

The W_L/W_E quantity, derived from the stress–strain curves

Table 2
The total work of viscoelastic deformation under drawing the PVP–PEG blends to a fixed elongation of $\varepsilon = 3$ (W_T), the work of elastic strain recovery in the course of retraction (W_E), their difference, characterizing the amount of lost energy (W_L), relevant contribution of elastic straining to the total deformation work (W_E/W_T), the W_L/W_E ratio, and the characteristics of polymer endurance in the course of extension/retraction cyclic straining, defined as a ratio of the total or elastic work in every subsequent cycle (n) to that in preceding ($n-1$) cycle (W_n/W_{n-1})

System	Cycle no.	W_T (MJ/m^3)	W_E (MJ/m^3)	W_L (MJ/m^3)	W_E/W_T	W_L/W_E	$W_{T_n}/W_{T_{n-1}}$	$W_{E_n}/W_{E_{n-1}}$
PVP–PEG (36%) 3.5% H_2O	1	1.872	0.959	0.913	0.512	0.952	–	–
PVP–PEG (36%), 4.5% H_2O	1	1.652	0.892	0.760	0.540	0.851	–	–
	2	1.109	0.718	0.391	0.648	0.544	0.671	0.806
	3	0.940	0.636	0.304	0.677	0.477	0.849	0.884
PVP–PEG (36%), 6.5% H_2O	1	1.278	0.769	0.509	0.602	0.662	–	–
	2	0.877	0.609	0.268	0.694	0.440	0.686	0.792
	3	0.734	0.525	0.209	0.715	0.389	0.837	0.862
PVP–PEG (36%), 11% H_2O	1	0.529	0.290	0.239	0.547	0.824	–	–
	2	0.330	0.224	0.106	0.679	0.473	0.623	0.773
	3	0.272	0.194	0.078	0.712	0.402	0.826	0.866
PVP–PEG (31%), 4.5% H_2O	1	9.107	0.864	8.243	0.095	9.541	–	–
	2	3.061	0.734	2.327	0.240	3.170	0.336	0.850
	3	0.556	0.140	0.416	0.252	2.971	0.182	0.191
PVP–PEG (41%), 4.5% H_2O	1	0.607	0.283	0.324	0.466	1.145	–	–
	2	0.314	0.186	0.128	0.591	0.688	0.518	0.657
	3	0.074	0.046	0.028	0.624	0.609	0.234	0.247

shown in Figs. 13–15, indicates how much the viscous, dissipated energy dominates the elastic energy, stored during an extension–retraction cycle. Like the tan $\delta = G''/G'$ value, a critical case is $W_L/W_E = 1$, when the dissipated energy is fully equated by the stored work. However, the W_L/W_E quantity relates to a large strain behavior of PVP–PEG blends, whereas the tan δ value, shown in Figs. 1, 6, and 7, characterizes a small strain behavior of the same systems in linear-elastic region. At $W_L/W_E > 1$ the polymer behaves mainly as a plastic. If $W_L/W_E < 1$, the rubber-like behavior is predominant.

As is obvious from the data in Fig. 16 and Table 2, the W_L/W_E curves pass through a minimum at 36% PEG concentration and 6.5% hydration. Although the effects of water and PEG on the viscous/elastic ratio are qualitatively similar, the impact of PEG is much stronger. Actually, at

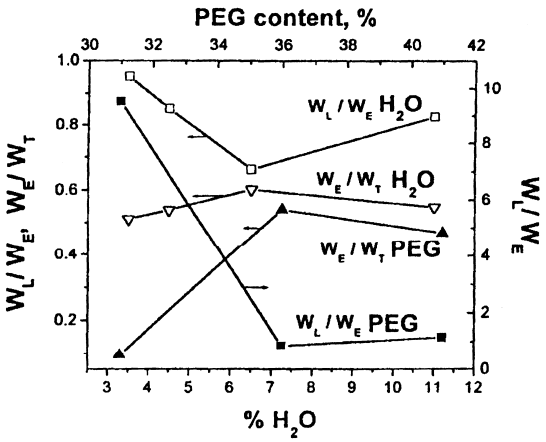

Fig. 16. Effect of PEG content and the concentration of sorbed water on the values of elastic contribution to the total work of viscoelastic deformation, W_E/W_T, and a viscous/elastic ratio, W_L/W_E, for the first extension–retraction cycle.

any hydration level the PVP blends with 36% PEG may be rather defined as predominantly elastomers ($W_L/W_E < 1$). At the same time, the PVP blend with 31% PEG may be unequivocally defined as a solid plastic, which exhibits a brittle-like behavior in the first extension cycle (see Fig. 15) and is characterized with enormous W_L/W_E value ($W_L/W_E = 9.541$). As the PEG content is increased up to 41% PEG, the blend behaves as a viscous liquid (see Fig. 15), $W_L/W_E = 1.145$. Note that in Fig. 16 the W_L/W_E value as a function of PEG content refers to the right, large-scale axis, while all other curves relate to the left axis. With increasing number of extension–retraction cycles, the curves drop toward lower W_L/W_E values. As a result, in the third cycle the W_L/W_E value tends to 2.971 and 0.609 for 31 and 41% PEG content, respectively (see Table 2).

For proper characterization of the effect of polymer 'training' in the process of cyclic extension–retraction deformation, the employment of a reproducibility factor is useful, defined as a ratio of the total or elastic work in subsequent, (n) cycle, to that in preceding, ($n-1$) cycle (W_n/W_{n-1}). If the W_n/W_{n-1} factor is 1, no irreversible energy dissipation occurs in the course of cyclic straining. Thus, the $W_{T_n}/W_{T_{(n-1)}}$ factor characterizes a polymer endurance, or resistance to irreversible expenditure of the total viscoelastic energy of straining under subsequent cyclic extensions. Accordingly, the $W_{E_n}/W_{E(n-1)}$ factor outlines polymer resistance to irrecoverable loss in elastic energy during subsequent cyclic retractions. As follows from the data presented in Table 2, a maximum irreversible energy consumption is observed during the first extension. For this reason, the W_3/W_2 values are always higher than the W_2/W_1 factor, and the reproducibility of elastic energy expenditures, relating to the retraction process, are always greater than those for the total energy of viscoelastic strain

under extension. Polymer structure orientation occurs mainly in the course of the first extension, and the first retraction as well as following strain cycles involve already initially oriented, or trained polymer. As is seen from Fig. 17, water does not affect appreciably the polymer resistance toward cyclic straining, in contrast to PEG behavior that impacts dramatically the W_n/W_{n-1} factor. With the rise of PEG concentration, the W_n/W_{n-1} factor increases for the blends possessing higher T_g values (Fig. 2) and insufficient molecular mobility within PEG content region between 31 and 36%. Let us recall, that in this region the short-chain PEG acts both as plasticizer and the enhancer of cohesive strength due to crosslinking PVP macromolecules by H-bonding through both terminal hydroxyl groups (see discussion around Fig. 10). At PEG concentrations higher than 36%, the PEG acts only as plasticizer and decreases the tolerance of PVP–PEG hydrogel to subsequent cyclic straining (Fig. 17). It is important to emphasize, that the system exhibiting the best pressure sensitive adhesion (36% of PEG [27,28]) is most tolerant to cyclic straining.

3.7. Tensile stress–strain behavior of PVP–PEG system in comparison with that of crosslinked rubber

Rubberlike behavior is typified by a low initial modulus (10^{-1}–10^{1} MPa) and a high tensile strain at break (commonly from several hundreds to 1–3 thousands percents) with the strain being to a large extent reversible. Qualitatively, the behavior of the PVP–PEG systems has been shown to obey this definition, but for more quantitative consideration it is helpful to compare the stress–strain curves up to break of the PVP–PEG blends with the tensile stress–strain relationship of a rubberlike network of a similar small-strain modulus, E.

The equilibrium stress–strain dependence of elastomeric networks was developed in a number of works [47–49]. The only parameter of the theory is the shear modulus, which due to incompressibility of the network is $G = E/3$. The latter determines the initial slope of the stress–strain curve. In the terms of true tensile stress $\sigma_{T,}$ relevant equation of rubberlike elasticity is:

$$\frac{\sigma_T}{E} = \frac{1}{3}\left[(\varepsilon+1)^2 - \frac{1}{\varepsilon+1}\right] \quad (3)$$

Eq. (3) describes satisfactorily the stress–strain curves of slightly crosslinked rubbers at comparatively low elongation values. In the region of intermediate elongations the experimental curve runs usually below the theoretical because the physical entanglements of long polymer chains, trapped between crosslinks, are able to slide under applied tensile stress and behave as slip-links. This leads to the decrease in reduced stress [49]. Under large elongations of crosslinked rubbers the experimental stress increases usually much steeper than the Eq. (3) predicts as a result of finite extensibility of polymer chains that is reached at high stretching.

Fig. 18 shows the effect of drawing rate on the strain dependence of true tensile stress normalized by the corresponding tensile modulus, which is calculated at $\varepsilon \rightarrow 0$. The agreement between experimental and theoretical curves in only reasonable under small elongations ($\varepsilon \leq 1$). Note that the $\varepsilon \approx 0.5$–1 corresponds to the onset of the elongational flow of the PVP–PEG blends (Figs. 3, 8, and 9), which in turn occurs upon the orientation of long PVP chains along the direction of stretching. In the stress–strain curves obtained in the course of probe tack test, the region of $\varepsilon = 0.5$–1.0 has been shown to correspond to the peak in debonding stress, when the cavitation and fibrillation of adhesive film occurs [28]. Under larger deformations, the PVP–PEG blend is always softer than the crosslinked rubber characterized with the same small-strain tensile modulus, E. Also, the higher the strain rate, the closer the behavior of PVP–PEG hydrogel to that of crosslinked rubber. Effect of increasing blend hydration is identical to the decrease in deformation rate (the data are not shown). In

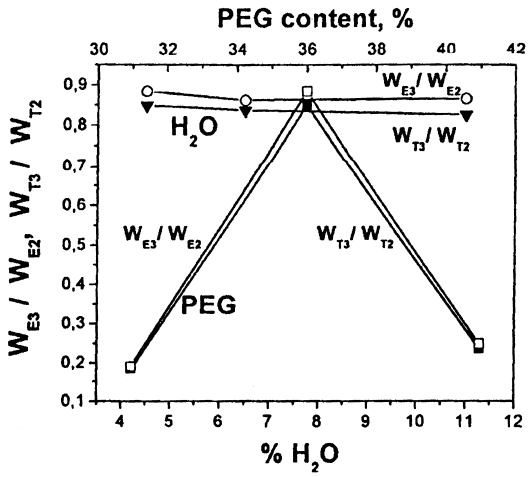

Fig. 17. Effect of PEG and water content on the tolerance of PVP–PEG blends to cyclic straining (W_{T3}/W_{T2}), and on the storage of elastic energy (W_{E3}/W_{E2}) between the third and the second extension–retraction cycles.

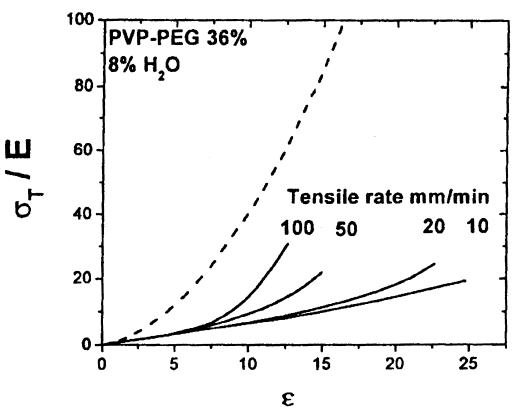

Fig. 18. Effect of drawing rate on the tensile strain dependence of true tensile stress, normalized by the small-strain modulus, σ_T/E, for PVP blend with 36% PEG containing 8% of sorbed water. The dash line outlines the equation of rubber elasticity (3).

a similar manner, increasing PEG content causes the rise in hydrogel compliance, much as the decrease in drawing rate.

As is evident from the curves shown in Figs. 18 and 19, the specific feature of the PVP–PEG systems, distinguishing its behavior from that of crosslinked rubber, is that the experimental stress never exceeds the value predicted with Eq. (3). This means that the large-strain behavior of the PVP–PEG system is characterized with tensile modulus, which is much smaller than the Young modulus, E, measured at $\varepsilon \rightarrow 0$. Such a behavior is not the case for any crosslinked rubbers and implies that the molecular mechanism of the break of PVP–PEG film does not most likely involve the limiting extension of PVP chains and the rupture of covalent bonds in the PVP backbone.

3.8. Proposed molecular mechanism underlying the stress–strain behavior of PVP–PEG adhesive hydrogel up to break

Fig. 20 shows schematically our idealized view of the mechanism of PVP–PEG hydrogel deformation in the process of uniaxial drawing. Long, linear polymers (like PVP) are believed to become entangled in interlinked loops that behave as a pseudo crosslinks, which, though they will eventually disentangle under drawing stress, contribute to long retardation times and high steady-flow viscosity. The addition of diluents (such as liquid oligomeric PEG or water in our case) reduces the number of entanglements per unit volume and increases long-term compliance and flow. Hydrogen bonding between two terminal PEG hydroxyls and the carbonyls in PVP repeating units has an effect on ductility similar to that of PVP chain entanglements. In concentrated PVP solutions in PEG-400, two different polymer networks are present. The first network is formed by the PVP chain entanglements, and the second one—by the PVP–PEG hydrogen bonding [20]. Adequate deconvolution of the contributions of these networks to the hydrogel modulus is difficult, however, the times required for the disentanglement of PVP chain are expected to be much

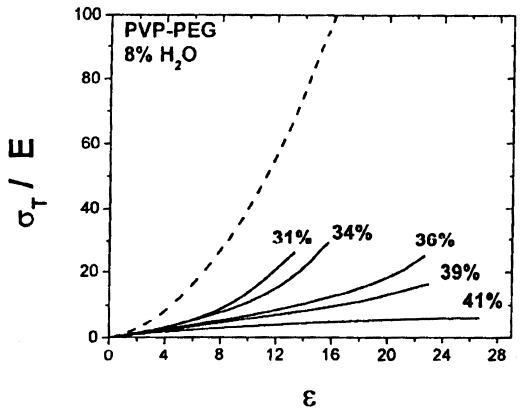

Fig. 19. Effect of PEG content on the tensile strain dependence of true tensile stress, normalized by the small-strain modulus, σ_T/E, for PVP–PEG blends containing 8% of sorbed water. Drawing rate is 20 mm/min. Dash line outlines the equation of rubber elasticity (3).

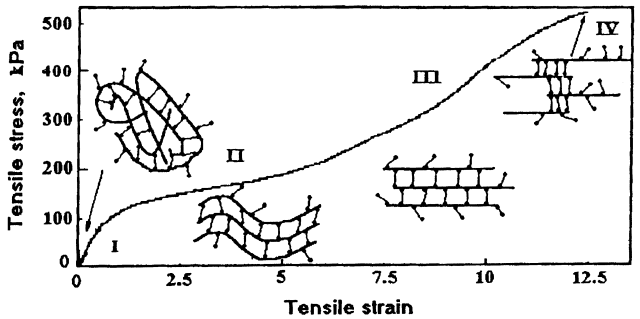

Fig. 20. Schematic presentation of an idealized mechanism of structural rearrangements within PVP–PEG adhesive blend in the course of uniaxial drawing to break.

longer than those associated with the rearrangement of the H-bonded network.

Indeed, the hydrogen bonds, which are destroyed under applied mechanical stress, may be quickly replaced by new ones in the course of stretching. Thus, we suppose that the PVP chain entanglements contribute mainly to the small-strain behavior (region I, Fig. 20), whereas the PVP–PEG H-bond crosslinking affects predominantly the resistance to elongational flow and hydrogel ductility within a steady-state region II (Fig. 20). The transition between regions I and II in the stress–strain curves is associated with the orientation of long PVP chains along the direction of stretching (evidenced by the appearance of optical anisotropy in polarized light), the fibrillation of the adhesive film (observed in the course of probe tack testing [28]), and with the onset of elongational flow.

The strain hardening effect and a transition from the region II to region III (Figs. 20) is thought to be associated with a phase segregation within the PVP–PEG adhesive hydrogel under tensile stress. This is only the case for hydrogel stretching with a high drawing rates (50 and 100 mm/min or higher), and never occurs for PVP–PEG film uniaxial extension with a low rate of 10 mm/min, when the H-bonds network is allowed to relax appreciably during the deformation process, and the mechanical stress is comparatively low. The hypothesis of phase segregation within the strain hardening region III under a high tensile stress is evidenced by our observations, which are as follows:

1. Uniaxially stretched film loses its optical transparency and becomes non-tacky. It is worthy of note, that similar effect has been also observed under adhesive debonding of the PVP–PEG hydrogel [27]. While the loss of transparency is a logical consequence of the fibrillation of adhesive film, the concomitant phase separation cannot be ruled out.
2. This phenomenon cannot be explained by the occurrence of crystallization processes, as has been established by a wide angle X-ray scattering technique [50].

It is known, that under a high mechanical stress compatible polymer blends can become immiscible and demonstrate a phase separation [51]. Because no weight loss is documented in this work for broken films upon their drawing, we suppose that it is the PEG-400 rather than water, which evolves into a separate phase. These observations need further investigation.

While the hydrogen bonding affects appreciably the polymer behavior under uniaxial drawing, in turn, the elongational flow of the polymer mixture affects the mechanism of H-bonding. As has been recently shown by Dormidontova and ten Brinke [52], besides the orientation of associating polymer chains along the flow direction, their stretching occurs (see Fig. 20). If the former factor facilitates the elongational flow, the latter impedes it and contributes appreciably to strain hardening.

Finally, as a microscopy of the sample in the course of elongation has established, within the region IV (Fig. 20) the fibrils of PVP–PEG hydrogel elongate to a limiting degree of ε_b and fail cohesively. Similar fracture mechanisms, involving the fibrillation of stretched adhesive, have been also established to characterize the PVP–PEG hydrogel adhesive joints failure in the process of both the peel [27] and probe tack tests [28]. Since the failure occurs always through the rupture of loosest bonds, and H-bonds are much looser than the covalent bonds, we believe that rather the pullout of long PVP chains from the stretched fibrils underlies the mechanism of the break of PVP–PEG film under uniaxial extension than the rupture of covalent bonds in the PVP backbones. In this way, the ultimate stress, σ_b, is supposed to be proportional to the total energy of ruptured hydrogen bonds, which held together the stretched PVP chains within the fibrils (see Fig. 20).

Taking into account the transient character and fast reformation of the H-bonded network, we believe that under slow extension the intermolecular H-bonds in PVP–PEG blends have time to rupture and reform anew at another place during deformation and do not contribute appreciably to the resistance to strain until the onset of critical, strain hardening region III, where the final rupture of H-bonded crosslinks between the PVP chains occurs (IV, Fig. 20). In contrast, at higher extension rates the H-bonds have insufficient time for rearrangement at new places and behave like pseudo cross-links, which have to be ruptured in order to deform the polymer. The narrow transition from ductile to tight stretching with the rise of drawing rate in Fig. 3 corresponds to a well-defined rate of the rearrangement of H-bonded network under drawing the PVP–PEG adhesive. Assuming that breakup and reformation of hydrogen bonds forming PVP–PEG network can occur below the critical deformation rate of $0.05\ s^{-1}$ we can identify the characteristic time for this process to occur at about 20 s. The sharp transition between the ductile and tight deformation modes with the change in extension rate is featured only for H-bonded PVP–PEG system and untypical of SIS and PIB based adhesives (compare Figs. 3 and 4).

Since the PEG has been shown to act mainly as plasticizer at small deformations and as the enhancer of cohesive strength at large deformations (Section 3.5, Figs. 8 and 10), this means that the contribution of the hydrogen bonded network is most pronounced under intermediate and large straining. At this stage the H-bonds are broken and reformed, and hydrogel flows like the yield stress liquid. At the same time, at small strains the H-bonded network gives a very high stiffness to the material, which is much greater than what could come from the entanglements of PVP chains.

The existence of these two very different mechanisms is illustrated by the impossibility to fit experimental stress–strain curves with either the equation of rubber elasticity (Eq. (3)) or by the flow of polymer fluid. Because the H-bonded crosslinks provided by the short PEG chains are able to slide along the longer and oriented in parallel the PVP chains (Fig. 20), this leads to the decrease in tensile stress, and the a material is much softer than crosslinked rubbers. This slip-crosslink mechanism of the deformation is valid both at intermediate and large strains. This mechanism underlies also the cohesive failure of stretched PVP–PEG fibrils and explains why the measured ultimate stress is always lower than the value predicted with the equation of rubber elasticity (3).

4. Conclusions

Solutions, or single-phase blends of PVP and liquid PEG of disparate chain lengths display a narrow concentration region, wherein a range of unique physical properties is observed. Among such properties are the occurrence of two glass transition temperatures and pressure sensitive adhesion, which are featured only in this narrow region of compositions. Mechanical properties examined throughout this concentration region show a pronounced decoupling between the small-strain and large-strain behaviors. Such decoupling is due to the existence of two types of network in PVP–PEG blends. The first network is mainly provided by physical entanglements of longer PVP chains and contributes mainly to the material behavior under small deformations. The second network is associated with much shorter and flexible chains of PEG, and is formed by hydrogen bonding of two terminal hydroxyl groups of the PEG of complementary carbonyl groups in monomer units of PVP. Due to the location of H-bonding groups at both ends of PEG chains, the PEG acts as a crosslinker of PVP macromolecules. Due to the flexibility of PEG chains, they couple the PVP crosslinking and an enhancement of cohesive toughness with formation of a large free volume and plasticization effect. Since the PVP–PEG H-bonded network complex has been earlier shown to be stoichiometric, at PEG contents 36% and less, the PEG behaves

mainly as the enhancer of cohesive toughness by forming reversible crosslinks with the PVP chains. In contrast, at PEG concentrations more than 36%, the PEG acts mainly as plasticizer. As is reported above, this molecular mechanism of PVP–PEG interaction underlies the mechanical properties of their blends.

Indeed, the twofold effect of PEG is well illustrated, for example, by the compositional behavior of the ultimate tensile strength, σ_b (Fig. 10). Another particular feature of the hydrogen bonded PVP–PEG network is the existence of a well-defined time for its structural rearrangement, which in turn depends upon the life-time of H-bonds under applied mechanical stress. Under slow drawing rates, the PVP–PEG hydrogel behaves as a ductile, uncrosslinked elastomer, whereas at faster extension rates it deforms and breaks as a tight, cured rubber. The transition from the ductile to the tight stretching mode occurs in a narrow range of deformation rates. In exactly the same manner, the type of extension changes from ductile to tight with a very small decrease in the concentration of both plasticizers in blend—PEG (between 36 and 34%, Fig. 8) and water (between 6.5 and 3%, Fig. 9). The measured Young's modulus (that relates to the linear-elastic region under small strains) and the σ_b/ε_b ratio (which defines the polymer break under large elongations) is only of comparable magnitude in the course of slow uniaxial drawing of PVP blends with 36% PEG (Table 1). This implies that the PVP–PEG blends are closer to a rubber-like behavior if the deformation time is longer than the time required to rupture H-bonds and reform them at another place in the course of elongational flow. And actually, as is evident from the data presented in Section 3.8 of this paper (Fig. 16), the contribution of recoverable, elastic work to the total work of viscoelastic deformation of PVP–PEG blends is predominant under slow extension and achieves the value of 70% for the PVP blends with 36% PEG. At the same time, the blend containing 31% PEG represents a solid plastic, whereas at 41% PEG the material flows like a viscous liquid. In this way, the PVP blend with 36% PEG provides the best viscoelastic properties needed for its application as pressure sensitive adhesive.

Acknowledgements

The research of Russian team was in part made possible by Award No. RC1-2057 of the US Civilian Research and Development Foundation (CRDF) and by support of the Corium International, Inc. We thank Acad. N.A. Plate, Prof. V.E. Dreval and Dr E.E. Dormidontova for helpful discussion and comments.

References

[1] Satas D, editor. Handbook of pressure-sensitive adhesive technology, 3rd ed. Warwick, Rhode Island: Satas, Associates; 1999.
[2] Gay C, Leibler L. Phys Today 1999;52(11):48–52.
[3] Gent AN, Schultz J. J Adhes 1972;3:281–94.
[4] Zosel A. J Adhes 1989;30:135–49.
[5] Verdier C, Piau JM, Benyahia L. CR Acad Sci Paris 1996;739–46. t323 Serie IIb.
[6] Chang EP. J Adhes 1991;34:189–200.
[7] Chang EP. J Adhes 1997;60:233–48.
[8] Gibert FX, Allal A, Marin G, Derail C. J Adhes Sci Technol 1999;13: 1029–44.
[9] Derail C, Allal A, Marin G, Tordjeman P. J Adhes 1997;61:123–57.
[10] Benyahia L, Verdier C, Piau JM. J Adhes 1997;62:45–73.
[11] Tse MF, Jacob L. J Adhes 1996;56:79–95.
[12] Dahlquist CA. In: Patrick RL, editor. Treatise on adhesion and adhesives, vol. 2. New York: Dekker; 1969. p. 219–60.
[13] Chu SG. In: Satas D, editor. Handbook of pressure-sensitive adhesive technology, 2nd ed. New York: Van Nostrand Reinhold; 1989. p. 158–203.
[14] Dale WC, Paster MD, Haynes JK. In: Satas D, editor. Handbook of pressure-sensitive adhesive technology, 2nd ed. New York: Van Nostrand Reinhold; 1989. p. 65–111.
[15] Feldstein MM, Platé NA. In: Sohn T, Voicu VA, editors. NBC Risks, NATO Science Series: 1. Disarmament Technologies, vol. 25. Dordrecht: Kluwer Academic; 1999. p. 441–58.
[16] Feldstein MM, Tohmakhchi VN, Malkhazov LB, Vasiliev AE, Platé NA. Int J Pharm 1996;131:229–42.
[17] Feldstein MM, Raigorodskii IM, Iordanskii AL, Hadgraft J. J Controlled Release 1998;52:25–40.
[18] Bairamov DF, Chalykh AE, Feldstein MM, Siegel RA, Platé NA. J Appl Polym Sci 2002;85:1128–36.
[19] Bairamov DF, Chalykh AE, Feldstein MM, Siegel RA. Macromol Chem Phys 2003;203(18):2674–85.
[20] Feldstein MM, Lebedeva TL, Shandryuk GA, Kotomin SV, Kuptsov SA, Igonin VE, Grokhovskaya TE, Kulichikhin VG. Polym Sci 1999; 41(8):854–66.
[21] Feldstein MM, Lebedeva TL, Shandryuk GA, Igonin VE, Avdeev NN, Kulichikhin VG. Polym Sci 1999;41(8):867–75.
[22] Feldstein MM, Kuptsov SA, Shandryuk GA, Platé NA. Polymer 2001; 42(3):981–90.
[23] Feldstein MM, Roos A, Creton C, Dormidontova EE. Polymer 2003; 44(6):1819–34.
[24] Jean YC, Ying L, Siegel RA, Feldstein MM. Manuscript in preparation.
[25] Vartapetian RSh, Khozina EV, Kärger J, Geschke D, Rittig F, Feldstein MM, Chalykh AE. Colloid Polym Sci 2001;279(6):532–8.
[26] Vartapetian RSh, Khozina EV, Karger J, Geschke D, Rittig F, Feldstein MM, Chalykh AE. Macromol Chem Phys 2001;202: 2648–52.
[27] Chalykh AA, Chalykh AE, Novikov MB, Feldstein MM. J Adhes 2002;78:667–94.
[28] Roos A, Creton C, Novikov MB, Feldstein MM. J Polym Sci, Polym Phys 2002;40:2395–409.
[29] Kaelble DH. In: Satas D, editor. Handbook of pressure-sensitive adhesive technology, 3rd ed. Warwick, Rhode Island: Satas and Associates; 1999. p. 87–120.
[30] Gul VE, Kuleznev VN. Structure and mechanical properties of polymers, 4th ed. ; 1994. Moscow, Labyrinth; p. 175–76.
[31] Creton C, Leibler L. J Polym Sci, Polym Phys Ed 1996;34:545–54.
[32] Satas D. In: Satas D, editor. Handbook of pressure-sensitive adhesive technology, 3rd ed. Warwick, Rhode Island: Satas and Associates; 1999. p. 171–203.
[33] Roos A, Creton C. Proceedings of the 25th Annual Meeting Adhesion Society, Orlando, FL, USA; 2002. p. 371–3.
[34] Jagisch FC, Tancrede JM. In: Satas D, editor. Handbook of pressure-sensitive adhesive technology, 3rd ed. Warwick, Rhode Island: Satas and Associates; 1999. p. 346–97.
[35] Bamborough DW. In: Satas D, editor. Handbook of pressure-sensitive

adhesive technology, 3rd ed. Warwick, Rhode Island: Satas and Associates; 1999. p. 423–43.
[36] Satas D. In: Satas D, editor. Handbook of pressure-sensitive adhesive technology, 3rd ed. Warwick, Rhode Island: Satas and Associates; 1999. p. 706–23.
[37] Feldstein MM. Polymer 2001;42(18):7719–26.
[38] Feldstein MM, Chalykh AE, Platé NA. Proceedings of the Fifth European Conference on Adhesion (EURADH'2000), Lyon, France, September 18–21; 2000. p. 176–81.
[39] Feldstein MM, Shandryuk GA, Kuptsov SA, Platé NA. Polymer 2000; 41(14):5327–38.
[40] Feldstein MM, Kuptsov SA, Shandryuk GA. Polymer 2000;41(14): 5339–48.
[41] Feldstein MM, Kuptsov SA, Shandryuk GA, Platé NA, Chalykh AE. Polymer 2000;41(14):5349–59.
[42] Fox TG. Bull Am Phys Soc 1956;1:123.
[43] Feldstein MM, Chalykh AE, Vartapetian RSh, Kotomin SV, Bairamov DF, Borodulina TA, Chalykh AA, Geschke D. Proceedings of the 23rd Annual Meeting Adhesion Society, Myrtle Beach, SC, USA; 2000. p. 54–6.
[44] Ward IM. Mechanical properties of solid polymers. New York: Wiley; 1983. Chapter 2.
[45] Feldstein MM, Platé NA, Chalykh AE, Cleary GW. Proceedings of the 25th Annual Meeting Adhesion Society, Orlando, FL, USA; 2002. p. 292–94.
[46] Mullins L. Rubber Chem Technol 1957;30:555–71.
[47] Treloar LRG. The physics of rubber elasticity, 3rd ed. Oxford: Clarendon Press; 1975.
[48] Erman B, Mark JE. Structure and properties of rubberlike networks. New York: Oxford University Press; 1997.
[49] Meissner B. Polymer 2000;41:7827–41.
[50] Kuptsov SA. Personal communication.
[51] Chalykh AE, Gerasimov VK, Mikhailov YuM. Phase diagrams in polymer systems. Moscow: Yanus-K; 1998.
[52] Dormidontova EE, ten Brinke G. J Chem Phys 2000;113:4614–26.